



Research paper

Cell-type-specific imaging of neurotransmission reveals a disrupted excitatory-inhibitory cortical network in isoflurane anaesthesia



Juan Guo^{a,#}, Mingzi Ran^{a,#}, Zilong Gao^b, Xinxin Zhang^b, Dan Wang^a, Huiming Li^a, Shiyi Zhao^a, Wenzhi Sun^{b,c,*}, Hailong Dong^{a,*}, Ji Hu^{d,e,f,g,*}

^a Department of Anaesthesiology and Perioperative Medicine, Xijing Hospital, The Fourth Military Medical University, Xi'an 710032, China

^b Chinese Institute for Brain Research, Beijing 102206, China

^c School of Basic Medical Sciences, Capital Medical University, Beijing 10069, China

^d School of Life Science and Technology, ShanghaiTech University, Shanghai 201210, China

^e Shanghai Key Laboratory of Psychotic Disorders, Shanghai Mental Health Center, Shanghai 200030, China

^f Co-Innovation Center of Neuroregeneration, Nantong University, Nantong 226000, China

^g CAS Center for Excellence in Brain Science and Intelligence Technology, Shanghai 200030, China

ARTICLE INFO

Article History:

Received 16 December 2020

Revised 6 February 2021

Accepted 19 February 2021

Available online xxx

Keywords:

GABA glutamate neurotransmission anaesthesia consciousness cortex

ABSTRACT

Background: Despite the fundamental clinical significance of general anaesthesia, the cortical mechanism underlying anaesthetic-induced loss of consciousness (aLOC) remains elusive.

Methods: Here, we measured the dynamics of two major cortical neurotransmitters, gamma-aminobutyric acid (GABA) and glutamate, through *in vivo* two-photon imaging and genetically encoded neurotransmitter sensors in a cell type-specific manner in the primary visual (V1) cortex.

Findings: We found a general decrease in cortical GABA transmission during aLOC. However, the glutamate transmission varies among different cortical cell types, where in it is almost preserved on pyramidal cells and is significantly reduced on inhibitory interneurons. Cortical interneurons expressing vasoactive intestinal peptide (VIP) and parvalbumin (PV) specialize in disinhibitory and inhibitory effects, respectively. During aLOC, VIP neuronal activity was delayed, and PV neuronal activity was dramatically inhibited and highly synchronized.

Interpretation: These data reveal that aLOC resembles a cortical state with a disrupted excitatory-inhibitory network and suggest that a functional inhibitory network is indispensable in the maintenance of consciousness.

Funding: This work was supported by the grants of the National Natural Science Foundation of China (grant nos. 81620108012 and 82030038 to H.D. and grant nos. 31922029, 61890951, and 61890950 to J.H.).

© 2021 Published by Elsevier B.V. This is an open access article under the CC BY-NC-ND license (<http://creativecommons.org/licenses/by-nc-nd/4.0/>)

1. Introduction

General anaesthesia is widely applied in clinical practice, and the estimated number of surgical procedures worldwide exceeds 300 million each year [1]. However, the cortical mechanisms underlying anaesthetic-induced loss of consciousness (aLOC) remain elusive [2–4]. Previous studies have focused on the effect of anaesthetics on functional connectivity within the cortical network [5–13]. Unraveling the dynamics of neurotransmission is the foundation of understanding the precise functional connectomics within the cortical

network during aLOC [14]. To date, cortical neurotransmission has mainly been measured by *ex vivo* electrophysiology recording of receptor-mediated currents [15–18] or by *in vivo* microdialysis followed by quantification through high-performance liquid chromatography (HPLC) [19–21]. However, these methods generally lack cell-type specificity, and the spatiotemporal resolution needed to accurately dissect neurotransmitter transients in the complex cortical network during aLOC occurred transiently within tens of seconds.

The elaborate cortical network is mainly composed of excitatory pyramidal cells (PCs) and three molecularly distinct inhibitory interneurons expressing parvalbumin (PV), somatostatin (SOM), or vasoactive intestinal peptide (VIP) [22–27]. They form a complex cortical neural network through synaptic interconnections releasing gamma-aminobutyric acid (GABA) and glutamate. Facilitation of inhibitory transmission and suppression of excitatory transmission were once considered to be possible mechanisms underlying aLOC [28–30]. Notably,

* Corresponding authors.

E-mail addresses: sunwenzhi@cibr.ac.cn (W. Sun), hldong6@hotmail.com (H. Dong), hujishi@shanghaitech.edu.cn (J. Hu).

These authors contributed equally.

Research in context

Evidence before this study

General anaesthesia is widely applied in clinical practice, yet the cortical mechanisms by which general anaesthetics induce loss of consciousness (aLOC) remains unclear. Disrupted functional connectivity within the cortical network is implicated in aLOC. Cortical neurotransmission has mainly been measured by *ex vivo* electrophysiology recording and by *in vivo* microdialysis. There is little research on the *in vivo* cortical neurotransmission underlying general anaesthesia with cell-type specificity and high spatiotemporal resolution.

Added value of this study

Using *in vivo* two-photon imaging and genetically encoded fluorescent indicators, we systematically investigate the GABA/glutamate/calcium dynamics of the primary visual cortex with cell-type specificity during isoflurane anaesthesia. The cortical GABA transmission was generally decreased without cell-type specificity. Glutamate transmission varied among different cortical cell types: it was almost preserved in pyramidal cells and was significantly reduced in inhibitory interneurons. The activity of inhibitory interneurons exhibited a distinct response pattern during aLOC, with VIP interneurons showing delayed inhibition and PV interneurons displaying rapid and significant inhibition.

Implication of all the available evidence

These findings reveal a disrupted excitatory-inhibitory cortical network during aLOC and suggest that the inhibitory network plays a vital role in the maintenance of consciousness. Besides, this study provides new insight for understanding the mechanism of general anaesthesia.

as approved by the IACUC (20180605) at the Fourth Military Medical University and the IACUC (2020040700 [2]) at ShanghaiTech University.

2.2. Animals

The following mice (2–4 months old) were used in the experiments: *VIP-ires-Cre*, JAX Stock No. 010908; *PV-ires-Cre*, JAX Stock No. 008069; *SOM-ires-Cre*, JAX Stock No. 013044; and C57BL/6J, JAX Stock No. 000664. Mice were maintained on a 12 h day/12 h night cycle at a constant temperature (24 ± 2 °C) and humidity ($60 \pm 2\%$) with ad libitum access to food and water (the National Center for Protein Science, Shanghai).

2.3. Virus injection and chronic cranial window surgery

AAV vectors containing DIO-iGluSnFR and DIO-iGABASnFR were packaged into the AAV2/9 serotype with titres of $1-5 \times 10^{12}$ viral particles per ml. C57BL/6J mice were injected with the 1:1 virus mixture of AAV-CAMKII-cre with AAV-DIO-GCaMP6m, AAV-DIO-iGABASnFR, or AAV-DIO-iGluSnFR prepared on the day of injection. Inhibitory interneuron transgenic mice were directly injected with AAV-DIO-GCaMP6m, AAV-DIO-iGABASnFR, or AAV-DIO-iGluSnFR. Virus injection and chronic cranial window implantation procedures have been described previously [36]. Briefly, mice were anaesthetized with pentobarbital (100 mg/kg, i.p.) and mounted in a stereotaxic instrument [37–38]. Eye cream was applied to the eyes of mice to prevent dehydration. Under sterile surgical conditions, a small craniotomy (~2.5 mm diameter) was made over the V1 cortex (centre coordinate: 2.5 mm lateral and 2.5 mm posterior to bregma). Using a microsyringe pump (MO10), 30–50 nl/site of the viral solution was slowly injected into the V1 cortex (400 μ m below the pia). The craniotomy was then covered with a circular glass coverslip (2.5 mm diameter, Thermo Fisher Scientific, Germany) and fixed with Crazy Glue (Roti Coll-1, CarlRoth, Germany). A titanium head post was then implanted in the exposed skull with glue and cemented with dental acrylic (Paladur, Heraeus Kulzer, Germany). Two stainless steel screws for EEG recording were inserted into the left side of the skull and fixed with dental acrylic. *In vivo* imaging and EEG recording were carried out after 2–4 weeks of recovery and habituation for head fixation.

2.4. Two-photon imaging and EEG recording

Mice were placed on the head-fixation apparatus. Anaesthesia was induced and maintained by 1.2% isoflurane with pure O₂ at a flow rate of 1 L/min. During anaesthesia, two-photon and EEG signals were recorded at the same time. The calcium, GABA, and glutamate activity of layer 2/3 (~60–280 μ m below the pia) neurons in the V1 was imaged using a Scientific two-photon laser scanning microscope [36]. The intensity of the excitation from a tunable femtosecond laser (Coherent Ultra II) was controlled by a Pockel Cell. The excitation laser was focused using a 20x/1 NA water immersion objective. Cells labelled with genetically encoded fluorescence indicators AAV-GCaMP6m, AAV-iGABASnFR, and AAV-iGluSnFR were excited at 920 nm at approximately 60 mW. Green emitted fluorescence was collected through a 50 nm bandpass filter centred at 525 nm. Frames of 512×512 pixels (approximately 440 μ m \times 380 μ m) were acquired at ~31 Hz using resonant scanning. EEG signals were continuously recorded by a Powerlab 16/35 amplifier system (PL3516, AD Instruments, Australia) and LabChart software at a sampling frequency of 1000 Hz.

2.5. Immunohistochemistry

To confirm the specific expression of the genetically encoded indicators GCaMP6m, iGABASnFR, and iGluSnFR in pyramidal, PV, SOM,

newly developed genetically encoded fluorescent sensors of iGABASnFR [31] and iGluSnFR [32] have allowed tracking of the GABA and glutamate dynamics of the brain with high spatiotemporal resolution. Combined with two-photon fluorescence microscopy and transgenic Cre mice, the GABA and glutamate neurotransmission of specific cell types within the cortical network can be accessible under rapid brain state transitions, which would contribute to revealing the cortical excitatory-inhibitory network dynamics at the mesoscale during aLOC.

Here, we systematically investigated the GABA and glutamate dynamics of excitatory neurons and three major inhibitory neuron subtypes in layer 2/3 of the primary visual (V1) cortex during aLOC. We focused on the layer 2/3 of the cortex because it is a critical structure of intracortical information integration [33–35]. We found a general decrease in cortical GABA transmission during aLOC. However, the glutamate transmissions onto different cortical cell types are different, where in it is almost preserved onto pyramidal cells and is significantly reduced onto inhibitory interneurons. These data revealed an anaesthetic-induced cortical state with a disrupted excitatory-inhibitory network. In addition, the activity of inhibitory interneurons exhibited a distinct response pattern during aLOC, among which VIP interneurons showed delayed inhibition and PV interneurons showed rapid and significant inhibition, suggesting that a functional inhibitory network is indispensable in the maintenance of consciousness.

2. Methods

2.1. Ethics

Animal care and use strictly followed institutional guidelines and governmental regulations. All experiments were performed exactly

and VIP neurons, we performed glutamate/PV/SOM/VIP immunohistochemistry. The mice were deeply anaesthetized with pentobarbital and then transcardially perfused with saline followed by 4% paraformaldehyde (PFA) in PBS [37–40]. The brain was postfixed in 4% PFA for 2 h at 4 °C and then placed in 30% sucrose solution overnight. The V1 sections were cut into 40 μ m coronal slices using a cryostat (Leica, CM1900, Germany) and incubated for 2 h in blocking solution (5% bovine serum albumin and 0.3% Triton X-100 in PBS). Next, slices were incubated for 24–72 h at 4 °C with one of the following primary antibodies: 1:1000 dilution of anti-glutamate rabbit (#G6642, RRID: AB_259946, Sigma-Aldrich), 1:500 dilution of anti-parvalbumin rabbit (#ab11427, RRID: AB_298032, Abcam), 1:1000 dilution of anti-somatostatin rabbit (#T-4103, RRID: AB_518614, Peninsula Laboratories International, Inc.), or 1:500 dilution of anti-VIP rabbit (#20077, RRID: AB_572270, Immunostar, Inc.). After washing with PBS thoroughly, slices were stained with secondary antibody, Alexa Fluor 594 donkey anti-rabbit IgG secondary antibody (1:1000, Jackson ImmunoResearch), for 2 h at room temperature. Subsequently, slices were washed three times with PBS and mounted onto glass slides. Finally, confocal microscopy images were acquired with a Leica SP8 using 20x and 40x objectives. All images were analysed with ImageJ software.

2.6. Two-photon data pre-processing

Imaging stacks were analysed with custom programs written in MATLAB (Mathworks) [36]. Imaging data were first corrected for motion-induced frameshift in the x and y directions using a cross-correlation-based registration algorithm. Regions of interest (ROIs) were manually selected in Fiji. The averaged fluorescent signal within the ROI was used to calculate calcium transients. We calculated the activity of calcium, GABA, and glutamate as $\Delta F/F$ (%) = $(F - F_0)/F_0 \times 100$, where F_0 was determined by the mode of the fluorescence intensity histogram. The noise (neuropil) background was subtracted from every trace, and a digital smoothing filter was used to smooth the traces. Then, the data were used for further analysis. $\Delta F/F$ values of calcium, GABA, and glutamate are presented as average plots with a shaded area indicating s.e.m.

2.7. $\Delta F/F_{(Ana-awake)}$ and slope

To evaluate the activity of cortical neurons during anaesthetic-induced LOC, we sought out the minimum point after administration of isoflurane through the derivation of the $\Delta F/F$ of each neuron. $\Delta F/F_{ana}$ was the average value of $\Delta F/F$ within one minute centered on the minimum point. $Time_{ana}$ was the time of the minimum point. $\Delta F/F_{awake}$ was the average signal of the $\Delta F/F$ of each neuron within 3 minutes before the administration of isoflurane. $\Delta F/F_{ana1}$ was the average signal of the $\Delta F/F$ value within 1 min after isoflurane administration.

$$\Delta F/F_{(Ana-awake)} = \Delta F/F_{ana} - \Delta F/F_{awake}$$

$$\Delta F/F_{(Ana1-awake)} = \Delta F/F_{ana1} - \Delta F/F_{awake}$$

$$Slope = \Delta F/F_{ana}/Time_{ana}$$

$\Delta F/F_{(Ana-awake)}$ reflects the activity of cortical neurons during anaesthetic-induced LOC, and the slope represents the neuronal suppression level per unit time. We analysed the percentage of $\Delta F/F_{(Ana1-awake)} > 0$ of each subtype of cortical neurons.

2.8. Calcium events

To evaluate the specific calcium response pattern of inhibitory interneurons during anaesthetic-induced LOC, we calculated the 'calcium events' of the cortical neurons from 3–6 min after

administration of isoflurane. The baseline was determined by the mode of the $\Delta F/F$ histogram. The threshold was established by the $\Delta F/F$ of baseline plus five standard deviations. The extreme points above the threshold of $\Delta F/F$ trace (within 3–6 min after isoflurane administration) were processed with a digital Butterworth lowpass filter at 0.05 Hz. The number of extreme points and the sum of $\Delta F/F$ points above the threshold were defined as the 'calcium events' and 'total calcium activity'.

2.9. Correlation analysis

The $\Delta F/F$ traces were segmented into three intervals: the awake stage (corresponding to the interval within 3 min before isoflurane administration) and two isoflurane anaesthesia stages (iso-1 and iso-2, corresponding to the intervals of 0–3 min and 3–6 min after isoflurane administration, respectively). To evaluate neuronal synchrony under different stage, Pearson's pairwise correlation coefficient (Pearson's r) was computed between $\Delta F/F$ traces of neuron pairs within the same field of view (FOV). The cumulative percentage reported the correlation coefficient of population data within cell type (correlations were prefiltered for a significance level of $p < 0.05$). We analysed the percentage of r values > 0.4 for each subtype of cortical neurons.

2.10. EEG analysis

The spectrum and burst suppression ratio (BSR) of the raw data filtered at 0.3–250 Hz were generated with custom programs written in MATLAB. The method for BSR quantification has been described previously [41–42]. Briefly, the EEG with burst suppression waves was characterized by periods of isoelectric activity and high-voltage activity. The suppression wave was determined when the duration of isoelectric activity was above 0.5 s. The BSR was the percentage of suppression wave (by time) within 1 min. The spectral analysis was performed by the MATLAB signal processing toolbox based on previous methods [42–43]. The data were processed with a fast Fourier transform to provide the absolute power spectrum of the frequency band. The power of gamma frequency (γ : 25–150 Hz) per minutes was calculated within 3 min before and 10 min after isoflurane administration. The value γ -awake was quantified as the average gamma power before isoflurane exposure. To avoid individual differences, the gamma power of each minute was normalized with γ -awake as the benchmark.

$$Normalized_ \gamma = (\gamma - \gamma_{awake})/\gamma_{awake}$$

2.11. Statistical analyses

The t test, Mann-Whitney test, Wilcoxon test, Kruskal-Wallis one-way ANOVA, and Chi-square test were used to analyse the significance of the data. Parametric tests were used to analyse the data with Gaussian distribution, otherwise nonparametric tests were used. The corresponding statistical test is indicated in each figure and supplementary tables. In all cases, $p < 0.05$ was considered statistically significant. Asterisks denote statistical significance, * $p < 0.05$; ** $p < 0.01$; *** $p < 0.001$; **** $p < 0.0001$. Unless otherwise indicated, data are expressed as the mean \pm SD.

2.12. Role of the funding source

Financial support was provided by the National Natural Science Foundation of China. The funder of the study had nothing to do with the study design, data collection, data analysis, data interpretation, or writing of the report. The corresponding author had full access to all the data in the study and had final responsibility for the decision to submit for publication.

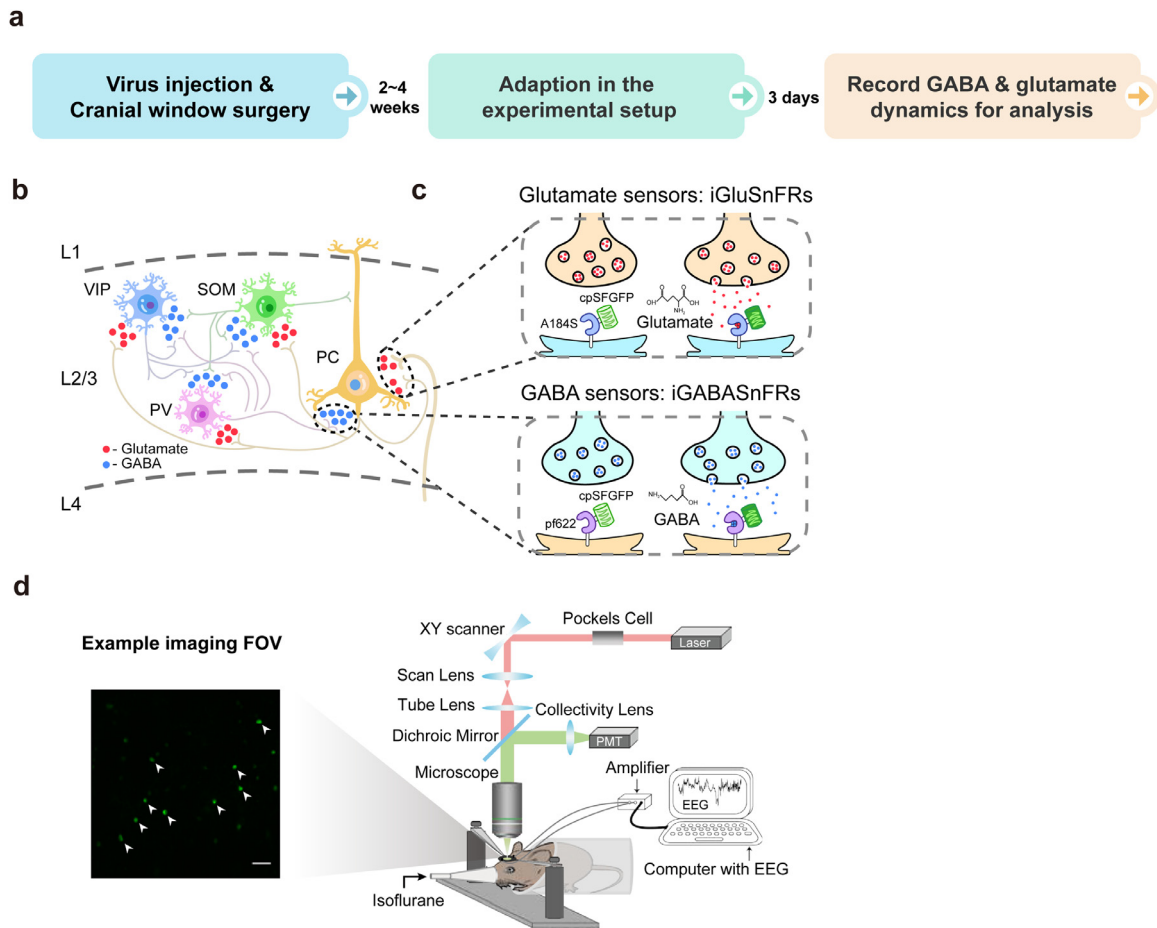


Fig. 1. *In vivo* chronic two-photon imaging of cortical GABA and glutamate dynamics with cell-type specificity during aLOC. **a** Core experimental procedures including virus injection, cranial window surgery, adaption, and recording process. **b** The GABA and glutamate input to the pyramidal, PV, SOM, and VIP neurons in layer 2/3 of the primary visual (V1) cortex. **c** Illustration showing the working mechanisms of iGABA-SnFR and iGluSnFR sensors. **d** Left image: a representative field of view (FOV) of iGABA-SnFR from a *VIP-ires-cre* mouse. Scale bar: 50 μ m. Right image: schematic of the experimental setup for two-photon imaging and EEG recording during isoflurane anaesthesia.

3. Results

3.1. *In vivo* chronic two-photon imaging of cortical GABA and glutamate dynamics with cell-type specificity during aLOC

To systematically examine the GABA and glutamate transmission dynamics of the cortical network during aLOC with cell subtype specificity and high spatiotemporal resolution, we used *in vivo* two-photon imaging (Fig. 1d) to record the GABA and glutamate dynamics of pyramidal cells as well as three major inhibitory neuron populations (PV, SOM, and VIP interneurons) in layer 2/3 of the V1 cortex during induction of isoflurane anaesthesia (Fig. 1b, c, and Fig. 2b). In this study, genetically encoded fluorescent indicators of iGABA-SnFR [31] and iGluSnFR [32] were used to report the transients of GABA and glutamate, respectively (Fig. 1c). We performed viral stereotactical injection and cranial window surgery of V1 in *C57Bl/6j*, *PV-ires-Cre*, *SOM-ires-Cre*, and *VIP-ires-Cre* mice to label pyramidal, PV, SOM, and VIP neurons. After 2–4 weeks of recovery and 3 days of adaption, mice were placed in a head-fixation apparatus (Fig. 1d, right panel) and administered 1.2% isoflurane in pure oxygen at a rate of 1 L/min through a customized plastic tube during the imaging process (Fig. 1a, also see Methods). 1.2% isoflurane can keep the mice in a stable unconscious state and minimize the impact on their hemodynamic and blood chemistry [10,44–45]. The GABA and glutamate activity of pyramidal, PV, SOM, and VIP neurons were dynamic during isoflurane-induced LOC, indicating the technical feasibility of GABA and glutamate imaging (Fig. 2c and Fig. 3b). The left panel of Fig. 1d

shows one representative imaging field of view (FOV). After the imaging process, we confirmed the specific expression of iGABA-SnFR and iGluSnFR in pyramidal, PV, SOM, and VIP neurons through immunofluorescence technology (also see Methods, Supplementary Fig. 2a, Fig. 3a, and Supplementary Fig. 4a).

In addition, we recorded the electroencephalogram (EEG) to assess the consciousness state during the induction of isoflurane (Supplementary Fig. 1a). Anaesthetic-induced loss and recovery of consciousness are closely associated with the attenuation and augmentation of electroencephalographic gamma activity [46–48]. Considering the individual differences in electroencephalographic gamma activity of mice during the awake state, we analysed the normalized gamma power during induction of isoflurane anaesthesia (also see Methods). In addition, the emergence of the burst suppression pattern of EEG is an indicator of brain transition from mild anaesthesia to deep anaesthesia [41]. The results showed a gradual reduction in normalized gamma power (Supplementary Fig. 1b) and ramping burst suppression ratio (BSR, Supplementary Fig. 1c) within 10 minutes after isoflurane administration. The normalized gamma power in the third minute after isoflurane administration was significantly decreased compared to that of the awake state (-0.64 ± 0.25 vs. 0 ± 0 , $n = 15$ mice, $H = 103.5$, $p = 0.0056$) (Supplementary Fig. 1b). The BSR at the fifth minute after isoflurane administration was significantly increased compared to that of the awake state ($8.95 \pm 11.16\%$ vs. $0 \pm 0\%$, $n = 15$ mice, $H = 81.9$, $p = 0.0007$) (Supplementary Fig. 1c). These results showed the stable brain state transition from awake to unconscious in mice in the custom-made isoflurane inhalation

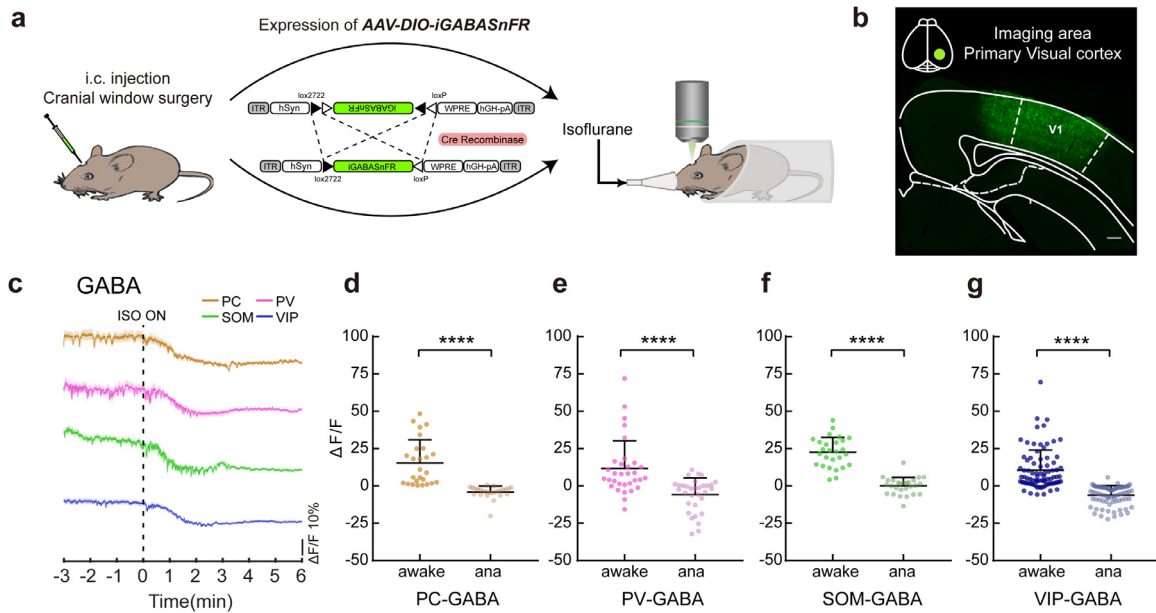


Fig. 2. Decayed GABA transmission onto each subtype of cortical neurons under anaesthesia. **a** Schematic of two-photon imaging after the expression of AAV-DIO-iGABASnFR following virus injection and cranial window surgery. **b** Virus expression in the imaging area of V1. Scale bar: 200 μm . **c** Signals of GABA input onto pyramidal (brown), PV (pink), SOM (green), and VIP neurons (blue) in response to isoflurane administration. Colour-shaded areas represent the respective s.e.m. **d-g** $\Delta\text{F}/\text{F}$ differences in pyramidal (**d**, $n = 26$ neurons from 7 mice), PV (**e**, $n = 32$ neurons from 5 mice), SOM (**f**, $n = 27$ neurons from 4 mice), and VIP (**g**, $n = 82$ neurons from 7 mice) neuronal GABA input between the awake state and anaesthetized state. Paired two-tailed Wilcoxon test (**d**, **e**, **g**) and paired two-tailed t test (**f**). Data with error bars are presented as the mean \pm SD, **** $p < 0.0001$.

apparatus. In summary, our experimental setup permits reliable, chronic *in vivo* two-photon imaging of cortical GABA and glutamate dynamics with cell-type specificity during isoflurane-induced LOC.

3.2. Decayed GABA transmission onto each subtype of cortical neurons under anaesthesia

We found that the GABA input onto each subtype of cortical neurons was immediately decreased upon administration of isoflurane (Fig. 2c). Within one minute of exposure to isoflurane, more than 80% of neurons within each subtype of cortical neurons received decreased GABA input (PC, 84.62% out of 26 neurons from 3 mice; PV, 93.75% out of 32 neurons from 5 mice; SOM, 92.59% out of 27 neurons from 4 mice; VIP, 96.12% out of 82 neurons from 7 mice) (Supplementary Fig. 2b). We analysed the maximum inhibitory degree of GABA transmission under isoflurane anaesthesia ($\Delta\text{F}/\text{F}_{\text{ana}}$, see Methods details). The results showed that isoflurane decreased the GABA input onto pyramidal ($W = -351$, $p < 0.0001$), PV ($W = -528$, $p < 0.0001$), SOM ($t = 12.42$, $p < 0.0001$), and VIP ($W = -3403$, $p < 0.0001$) neurons (Fig. 2d-g, Table S1). In addition, the decrease in GABA input signals ($H = 7.722$, $p = 0.052$) and the slope (the index of neuronal suppression level per unit time, $H = 5.527$, $p = 0.137$) of each subtype of cortical neurons were not significantly different across subtypes, suggesting that the GABA input to each subtype of the cortical neuron was decreased during isoflurane-induced LOC without cell type-specific effects ((Supplementary Fig. 2c,d, Table S2). These results demonstrate a general decayed GABA transmission under anaesthesia and suggest disrupted inhibitory neurotransmission within the cortical network during aLOC.

3.3. Preserved glutamate transmission to pyramidal cells during aLOC

The glutamate input to each subtype of cortical neurons also showed a downward trend upon the isoflurane administration (Fig. 3b). Compared with the awake state, the glutamate input onto pyramidal ($W = -300$, $p < 0.0001$), PV ($W = -1225$, $p < 0.0001$), SOM ($W = -406$, $p < 0.0001$), and VIP ($W = -3570$, $p < 0.0001$) neurons was decreased under isoflurane anaesthesia (Fig. 3c-f, Table S1),

suggesting disrupted excitatory neurotransmission within the cortical excitatory-inhibitory network during aLOC.

Interestingly, the decrease in glutamate input signals ($H = 26.66$, $p < 0.0001$) to pyramidal cells was smaller than that of inhibitory interneurons, and the slope ($H = 35.44$, $p < 0.0001$) of pyramidal cells was higher than that of inhibitory interneurons, indicating a tiny glutamate fluctuation of pyramidal cells compared to that of inhibitory interneurons during LOC (Fig. 3g,i, Table S3). The times ($H = 16.03$) needed for the maximum inhibition degree of pyramidal cells were longer than those for the inhibitory interneurons (Fig. 3h, Table S3). The results showed that glutamate dynamics vary among different cortical cell types during aLOC, in which glutamate is almost preserved on pyramidal cells and is significantly reduced on inhibitory interneurons.

The determinant of glutamate neurotransmission to inhibitory interneurons within L2/3 is mainly derived from pyramidal cells in the same layer [33]. We studied the activity of pyramidal cells within L2/3 of the V1 cortex under isoflurane anaesthesia (Supplementary Fig. 3a,b), and the results indeed showed a significantly decreased calcium activity ($W = -1081$, $p < 0.0001$) of pyramidal cells (Supplementary Fig. 3c,d, Table S1).

3.4. VIP neuronal calcium activity shows a delayed inhibition and a synchronized response pattern during aLOC

Inhibitory interneurons are the main source for delivering GABA within the local cortical network, among which VIP interneurons and PV/SOM interneurons specialize in disinhibitory and inhibitory control of pyramidal cells, respectively [24-25]. The maximum inhibitory effect of isoflurane anaesthesia on the GABA and glutamate input to inhibitory interneurons had no cell-type specificity (Supplementary Fig. 2c and Fig. 3g). Thus, we stereotactically infused AAV-DIO-GCaMP6m into the V1 cortex of PV-ires-Cre, SOM-ires-Cre, and VIP-ires-Cre mice to investigate whether the inhibitory interneurons present an identical response pattern under anaesthesia. Immunofluorescence confirmed the specific expression of the calcium indicator GCaMP6m in PV, SOM, and VIP interneurons (Supplementary Fig. 4b).

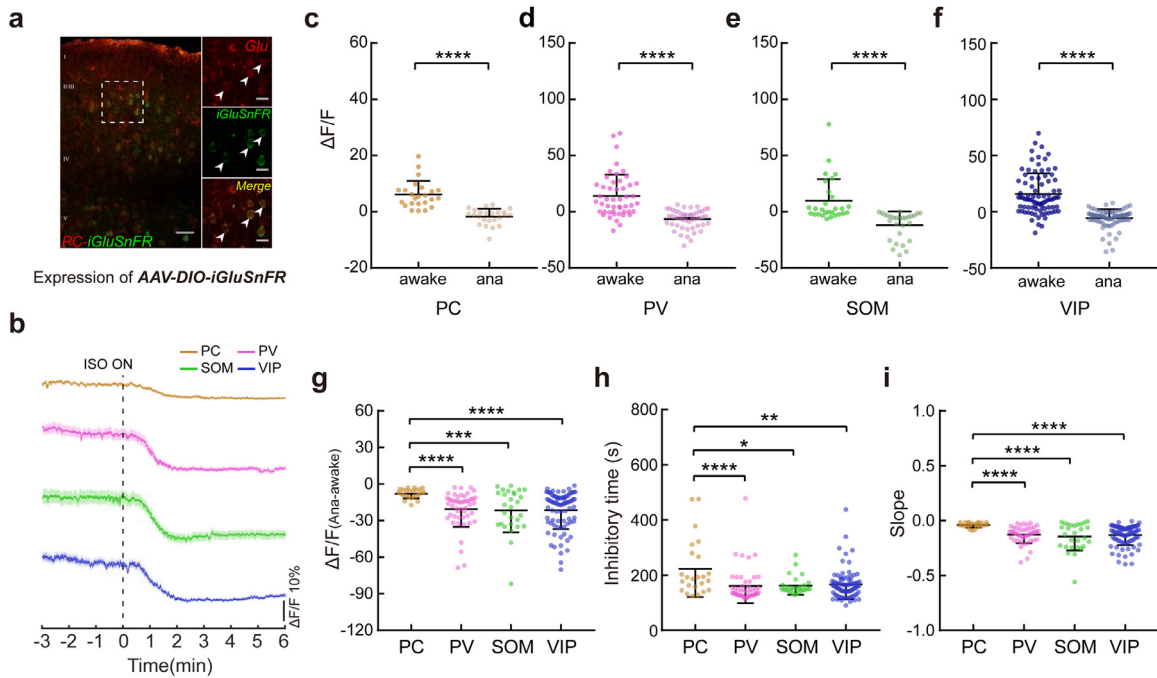


Fig. 3. Preserved glutamate transmission to pyramidal cells during aLOC. **a** Coexpression of iGluSnFR (green) and glutamate (red) within pyramidal cells in layer 2/3 of the V1 cortex. Scale bars: 50 μm (left) and 20 μm (right). Arrowheads indicate coexpressing cells. **b** Signals of glutamate input to pyramidal (brown), PV (pink), SOM (green), and VIP neurons (blue) in response to isoflurane administration. Colour-shaded areas represent the respective s.e.m. **c-f** $\Delta F/F$ difference in pyramidal (**c**, $n = 24$ neurons from 3 mice), PV (**d**, $n = 49$ neurons from 6 mice), SOM (**e**, $n = 28$ neurons from 4 mice), and VIP (**f**, $n = 84$ neurons from 7 mice) neuronal glutamate input between the awake state and anaesthetized state. Paired two-tailed Wilcoxon test. **g-i** The $\Delta F/F_{(\text{Ana-awake})}$ (**g**), inhibitory time (**h**), and slope (**i**) of pyramidal cells, PV, SOM, and VIP neurons. Kruskal-Wallis one-way ANOVA with Dunn's multiple comparisons. Data with error bars are presented as the mean \pm SD, * $p < 0.05$, ** $p < 0.01$, **** $p < 0.0001$.

However, the calcium signals of PV, SOM, and VIP interneurons under isoflurane-induced LOC exhibited distinct activity patterns (Fig. 4a). Within one minute of exposure to isoflurane, the average activity of VIP interneurons was the highest among the three kinds of interneurons ($H = 30.14$, VIP vs. SOM: $p = 0.0089$; VIP vs. PV: $p < 0.0001$) (Fig. 4b, Table S4). Approximately 54% of VIP interneurons presented higher activity than those in the awake state, and this ratio was higher than PV and SOM interneurons (VIP vs. SOM: $\chi^2 = 6.517$, $p = 0.0107$; VIP vs. PV: $\chi^2 = 19.71$, $p < 0.0001$) (Fig. 4c, Table S7). To demonstrate the specific calcium activity pattern of VIP interneurons during isoflurane-induced LOC, we quantified the 'calcium events' of each subtype of cortical neurons (also see Methods). The results showed that there were more calcium events in VIP interneurons than in PV and SOM interneurons ($H = 21.36$, VIP vs. SOM: $p = 0.0215$; VIP vs. PV: $p < 0.0001$) (Fig. 4d, Table S4). Similarly, the total calcium activity of VIP interneurons was stronger than that of the PV and SOM interneurons ($H = 32.82$, VIP vs. SOM: $p < 0.0001$; VIP vs. PV: $p < 0.0001$) (Fig. 4e, Table S4). These results indicated that the activity of VIP interneurons exhibited a delayed inhibitory response during aLOC.

Next, we calculated Pearson's linear correlation coefficient (r) of VIP neuronal pairs during awake (within 3 minutes before isoflurane administration) and two isoflurane anaesthesia stage (iso-1 and iso-2 are the 0–3 min and 3–6 min after isoflurane administration, respectively). As shown in Fig. 4f, VIP neuronal pairs showed a higher correlation profile during isoflurane anaesthesia. Compared with the awake state, the curve of r 's cumulative percentage was right-shifted (the aggregated data were prefiltered for a significance level of $p < 0.05$, Fig. 4g). The average r values during the iso-1 and iso-2 stages were higher than those during the awake state ($H = 114.7$, $p < 0.0001$) (Fig. 4h, Table S6). Further analysis showed that the percentage of r values above 0.4 during the iso-1 and iso-2 stages was higher than that during the awake state (awake vs. iso-1: $\chi^2 = 73.58$, $p < 0.0001$; awake vs. iso-2: $\chi^2 = 42.73$, $p < 0.0001$) (Fig. 4i, Table S7).

These results showed the elevated synchronization of VIP neuronal activity during aLOC.

3.5. Dramatic reduction in and high synchronization of PV neuronal calcium activity during aLOC

Moreover, the decrease in calcium signals of PV interneurons was larger than that of SOM interneurons ($U = 642$, $p < 0.0001$) (Fig. 5a, Table S5). There was no difference of the inhibitory time within these two types interneurons ($U = 1139$, $p = 0.3614$) (Fig. 5b, Table S5). The slope, which could represent the neuronal suppression level per unit time, of PV interneurons was lower than that of SOM interneurons ($U = 656$, $p < 0.0001$) (Fig. 5c, Table S5). These results suggested a dramatic reduction in PV neuronal activity.

PV and SOM neuronal pairs also showed higher synchronization under isoflurane anaesthesia (Fig. 5e,i). The average r values during the iso stage (0–3 min after isoflurane administration) were higher than that during the awake state (PV: $U = 4129$, $p < 0.0001$; SOM: $U = 13014$, $p < 0.0001$) (Fig. 5g,k, Table S6). Further analysis showed that the percentage of r values above 0.4 during the iso stage was higher than that during the awake state (PV: $\chi^2 = 157.5$, $p < 0.0001$; SOM: $\chi^2 = 38.31$, $p < 0.0001$) (Fig. 5h,l, Table S7).

In addition, the Pearson's r of PV interneurons was higher than that of SOM and VIP interneurons during induction of isoflurane anaesthesia ($H = 193$, PV vs. SOM: $p < 0.0001$; PV vs. VIP: $p < 0.0001$) (Fig. 5d, Table S6). These results indicated that each subtype of cortical neurons has a specific synchronization level during anaesthetic-induced unconsciousness, with PV interneurons being the most synchronized and SOM the least.

Together, these results showed that the activity of inhibitory interneurons is related to aLOC in a cell type-specific manner and suggested that a functional inhibitory network is indispensable in the maintenance of consciousness.

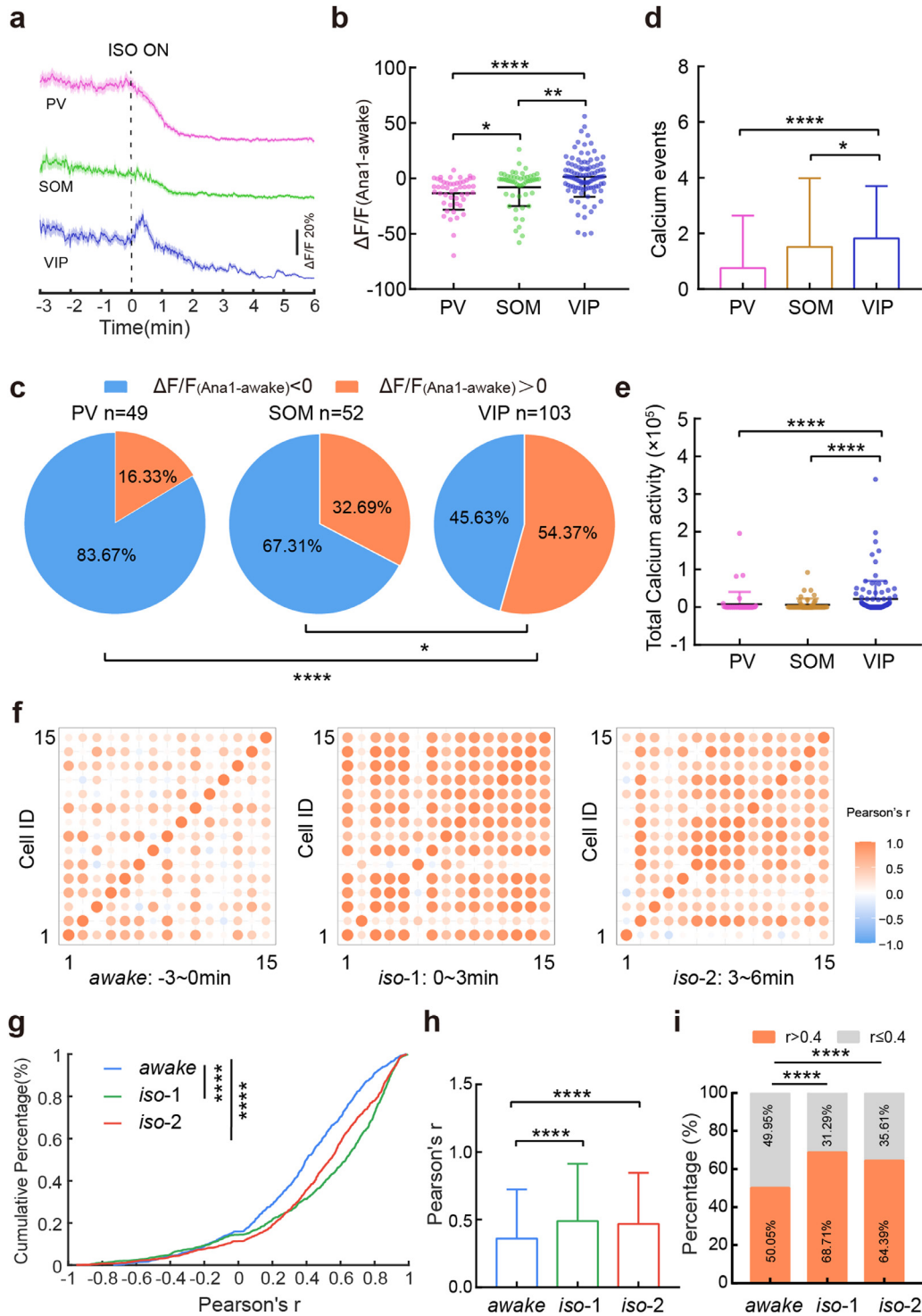
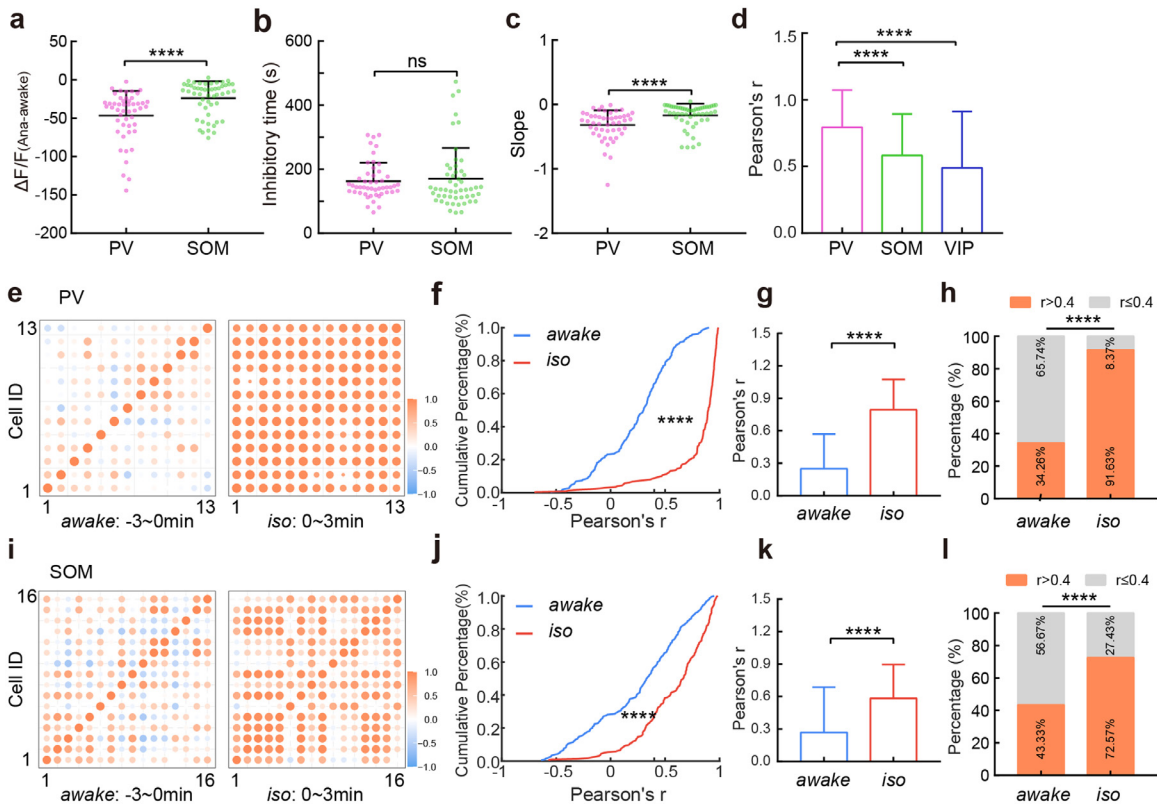


Fig. 4. VIP neuronal calcium activity shows delayed inhibition and a synchronized response pattern during aLOC. **a** Signals of calcium activity of PV (pink), SOM (green), and VIP (blue) neurons in response to isoflurane administration. Colour-shaded areas represent the respective s.e.m. **b** The $\Delta F/F_{(Ana1-awake)}$ of PV ($n = 49$ neurons from 5 mice), SOM ($n = 52$ neurons from 7 mice), and VIP ($n = 103$ neurons from 5 mice) neurons. $\Delta F/F_{(Ana1-awake)}$ refers to the difference in $\Delta F/F$ value within 1 minute after isoflurane administration minus $\Delta F/F$ value within the awake state before isoflurane administration. Kruskal-Wallis one-way ANOVA with Dunn's multiple comparisons. **c** The percentage of $\Delta F/F_{(Ana1-awake)} > 0$ within the PV, SOM, and VIP interneurons. Chi-square test. **(d, e)** The calcium events **(d)** and total calcium activity **(e)** of PV, SOM and VIP interneurons during the 3 to 6 minutes after isoflurane administration. Kruskal-Wallis one-way ANOVA with Dunn's multiple comparisons. **f** Matrix of correlation coefficient r of VIP neurons during awake and two isoflurane anaesthesia stages (0-3 minutes and 3-6 minutes after isoflurane administration). **(g, h)** Cumulative frequency distribution **(g)** and mean pairwise correlation **(h)** for Pearson's r of VIP neurons during awake and two isoflurane anaesthesia stages. Kruskal-Wallis one-way ANOVA with Dunn's multiple comparisons. **i** The percentage of $r > 0.4$ within VIP neurons during awake and two isoflurane anaesthesia stages. Chi-square test. Data with error bars are presented as the mean \pm SD, * $p < 0.05$, ** $p < 0.01$, *** $p < 0.001$, **** $p < 0.0001$.



4. Discussion

We combined *in vivo* two-photon imaging and genetically encoded fluorescent sensors [31–32] to investigate GABA and glutamate dynamics during aLOC. The results suggest that aLOC resembles a cortical state with a disrupted excitatory-inhibitory network (Fig. 6a,b).

Our results showed the isoflurane-induced globally decayed GABA input onto each cortical neuronal subtype (Fig. 6b). Isoflurane increased GABA A receptor-mediated neurotransmission in some nucleus other than cortex, such as vPAG [30], hippocampus [49–51],

and amygdala [52], etc. Consistent with previous studies [19–20], the present findings suggested that volatile anaesthetics did not facilitate GABA release within the V1 cortex and contributed to the understanding of the effect of isoflurane on the inhibitory neurotransmission. Glutamate is the main excitatory neurotransmitter in the cortex [53]. Using microdialysis technology, previous studies have reported different effects of anaesthetic on cortical glutamate dynamics, including increased glutamate concentration within the primary cortex [19] and unchanged glutamate within the prefrontal cortex [20]. Due to the limitation of spatiotemporal resolution, these results can reflect only the averaged glutamate level of the local neuronal

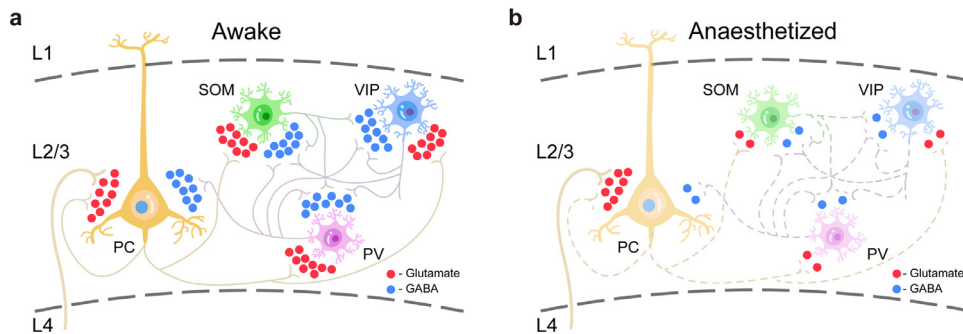


Fig. 6. Disrupted excitatory-inhibitory network within the V1 cortex during aLOC. **a** GABA and glutamate transmission of cortical pyramidal, PV, SOM, and VIP neurons during the awake state. **b** GABA and glutamate transmission within the cortical network during aLOC: general decayed GABA transmission onto each subtype of L2/3 cortical neurons which is mainly from the intralayer inhibitory interneurons; preserved glutamate transmission to L2/3 pyramidal cells which is mainly from the L4 pyramidal cells.

population under stable anaesthesia and are far from sufficient to reveal the glutamate transients during the induction of unconsciousness. Interestingly, our results showed diverse glutamate transients onto excitatory neurons and inhibitory interneurons during aLOC, in which glutamate transmission to pyramidal cells is relatively unchanged compared with the significant reduction to inhibitory interneurons (Fig. 6b). Pyramidal cells in L2/3 receive dense glutamate input from L4, and inhibitory interneurons receive dense glutamate input from the lateral projection of pyramidal cells within L2/3 [33–54]. Based on the anatomical connection of the local cortical network, our results indicated preserved feedforward glutamatergic signalling with cell-subtype specificity and layer specificity during anaesthetic-induced unconsciousness. Specifically, pyramidal cells rather than interneurons in L2/3 mainly receive feedforward glutamatergic input from L4 but cannot transmit this signal to downstream inhibitory neurons within L2/3 under anaesthesia. Overall, the results revealed a considerably richer picture of the preserved feedforward functional cortical connectivity and intracolumnar information disintegration during isoflurane anaesthesia.

Inhibitory interneurons are essential for maintaining cortical network dynamics [27]. The present results show that the activity of inhibitory interneurons exhibited a distinct response pattern during isoflurane-induced LOC. Interestingly, VIP interneurons have a specific delay inhibition pattern during the induction of unconsciousness. It has been reported that subcortical cholinergic transmission rather than glutamatergic transmission globally recruits cortical VIP interneurons during certain behavioural states [27–55]. Consistent with these findings, the present results showed that the activity of VIP interneurons during anaesthetic-induced unconsciousness is independent of glutamate input. There is one possibility that global recruitment of cortical VIP interneurons associated with subcortical cholinergic systems may play an essential role in the resistance of unconsciousness.

Sensory cortex is closely associated with the specific content of consciousness experience, primary visual cortex contributes to the neural processes underlying conscious visual perception [56–57]. Considerable evidence has revealed anaesthetic-induced unconsciousness is mainly associated with the disruption of the long-range cortico-cortical feedback connection and thus of destroyed cortical information integration [7–10]. Our results suggest the disconnected network [2] also occurred in the supragranular layer of the primary sensory cortex related to intracolumnar information integration. General anaesthesia does not decouple the pyramidal cells in the L2/3, which means they still could receive the feedback input even under anaesthesia [9]. In conjunction with the preserved glutamate and decayed calcium dynamics of pyramidal cells in this study, our findings offer a piece of indirect evidence for the disrupted feedback connectivity under anaesthesia which is a strong candidate mechanism for aLOC. In addition, unravelling the mechanism of anaesthesia is contributed to the development of new anaesthetics and the improvement of anaesthesia monitoring tools and safety.

There were also limitations of the study that should be considered. First, combining the transgenic mice and two-photon imaging, we acquired cell subtype-specific data with high spatiotemporal resolution from the L2/3 of the V1 cortex under isoflurane anaesthesia. However, the neuronal and network dynamics within other cortical areas and layers deserve further study to reveal the mystery of anaesthesia [58]. There is also a lack of neuro-behavioral measures to assess the isoflurane-induced unconsciousness. Second, the GABA and glutamate were decreased under anaesthesia, and unravelling how presynaptic exocytosis is affected could clarify the cortical mechanism of anaesthesia with greater precision [18–59–62]. Third, in addition to the neurotransmitters GABA and glutamate, neuromodulators correlated with anaesthesia, such as acetylcholine, dopamine, histamine, and serotonin, are also worth studying [20–63]. Finally, although previously conducted studies have reported that

almost all anaesthetics have a similar effect on certain cortical activities [2–9–64], further studies are still needed to investigate the multi-dimensional cortical network dynamics [65] under all kinds of anaesthetics given their diverse molecular and cellular targets.

In summary, our findings reveal a disrupted excitatory-inhibitory cortical network in isoflurane-induced unconsciousness and suggest an important role of the inhibitory network in maintaining consciousness.

Declaration of Competing Interests

The authors declare no competing interests.

Contributors

Conceptualization and verification of the underlying data, J.H., H. D., and J.G.; Methodology, W.S., J.G. and M.R.; Investigation, J.G., M.R., D.W., H.L. and S.Z.; Formal Analysis, J.G., W.S., Z.G., and X.Z.; Writing-Original Draft, J.G.; Writing-Review & Editing, J.H. and H.D.; Funding Acquisition, H.D. and J.H. All authors read and approved the final version of the manuscript.

Acknowledgments

We thank all members of the Hu and Dong labs. The authors thank Dr. Loren L. Looger for offering vectors of iGluSnFR and iGABASnFR. We also thank the staff members of the Molecular Imaging Core Facility (MICF)/Multi-Omics Core Facility (MOCF)/Biomolecular NMR Core Facility/Molecular and Cell Biology Core Facility (MCBCF) at the School of Life Science and Technology (ShanghaiTech University) and the Animal Facility at the National Facility for Protein Science (NFPS, Shanghai) for providing technical support. This work was supported by the grants of the National Natural Science Foundation of China (grant no. 81620108012 and 82030038 to H.D. and grant nos.31922029, 61890951, and 61890950 to J.H.)

Data sharing Statement

The data that support the findings of this study are available in the manuscript and from the corresponding author upon request (huji@shanghaitech.edu.cn).

Supplementary materials

Supplementary material associated with this article can be found, in the online version, at doi:10.1016/j.ebiom.2021.103272.

References

- [1] Rose J, Weiser TG, Hider P, Wilson L, Gruen RL, Bickler SW. Estimated need for surgery worldwide based on prevalence of diseases: a modelling strategy for the WHO Global Health Estimate. *The Lancet Global Health* 2015;3(Suppl 2):S13–20.
- [2] Wenzel M, Han S, Smith EH, Hoel E, Greger B, House PA, et al. Reduced Repertoire of Cortical Microstates and Neuronal Ensembles in Medically Induced Loss of Consciousness. *Cell Syst* 2019;8(5):467–74 e4.
- [3] Hudetz AG, Vizuete JA, Pillay S, Mashour GA. Repertoire of mesoscopic cortical activity is not reduced during anesthesia. *Neuroscience* 2016;339:402–17.
- [4] Lewis LD, Weiner VS, Mukamel EA, Donoghue JA, Eskandar EN, Madsen JR, et al. Rapid fragmentation of neuronal networks at the onset of propofol-induced unconsciousness. In: *Proceedings of the national academy of sciences of the United States of America*, 109; 2012. p. E3377–86.
- [5] Meyer K. The role of dendritic signaling in the anesthetic suppression of consciousness. *Anesthesiology* 2015;122(6):1415–31.
- [6] Luppi AH, Craig MM, Pappas I, Finoia P, Williams GB, Allanson J, et al. Consciousness-specific dynamic interactions of brain integration and functional diversity. *Nat Commun* 2019;10(1):4616.
- [7] Alkire MT, Hudetz AG, Tononi G. Consciousness and anesthesia. *Science* 2008;322(5903):876–80.
- [8] Pappas I, Adapa RM, Menon DK, Stamatakis EA. Brain network disintegration during sedation is mediated by the complexity of sparsely connected regions. *Neuroimage* 2019;186:221–33.

- [9] Suzuki M, Larkum ME. General anesthesia decouples cortical pyramidal neurons. *Cell* 2020;180(4):666–76 e13.
- [10] Redinbaugh MJ, Phillips JM, Kambi NA, Mohanta S, Andryk S, Dooley GL, et al. Thalamus modulates consciousness via layer-specific control of cortex. *Neuron* 2020;106(1):66–75 e12.
- [11] Barttfeld P, Uhrig L, Sitt JD, Sigman M, Jarraya B, Dehaene S. Signature of consciousness in the dynamics of resting-state brain activity. In: Proceedings of the national academy of sciences of the United States of America, 112; 2015. p. 887–92.
- [12] Li D, Vlisides PE, Kelz MB, Avidan MS, Mashour GA. Dynamic cortical connectivity during general anesthesia in healthy volunteers. *Anesthesiology* 2019;130(6):870–84.
- [13] Ishizawa Y, Ahmed OJ, Patel SR, Gale JT, Sierra-Mercado D, Brown EN, et al. Dynamics of Propofol-Induced Loss of Consciousness Across Primate Neocortex. *J Neurosci* 2016;36(29):7718–26.
- [14] Fornito A, Zalesky A, Breakspear M. The connectomics of brain disorders. *Nat Rev Neurosci* 2015;16(3):159–72.
- [15] Franks NP. General anaesthesia: from molecular targets to neuronal pathways of sleep and arousal. *Nat Rev Neurosci* 2008;9(5):370–86.
- [16] Kelly EW, Solt K, Raines DE. Volatile aromatic anesthetics variably impact human gamma-aminobutyric acid type A receptor function. *Anesth Analg* 2007;105(5):1287–92 table of contents.
- [17] Rudolph U, Antkowiak B. Molecular and neuronal substrates for general anaesthetics. *Nat Rev Neurosci* 2004;5(9):709–20.
- [18] Wang HY, Eguchi K, Yamashita T, Takahashi T. Frequency-dependent block of excitatory neurotransmission by isoflurane via dual presynaptic mechanisms. *J Neurosci* 2020;40(21):4103–15.
- [19] Dong HL, Fukuda S, Murata E, Higuchi T. Excitatory and inhibitory actions of isoflurane on the cholinergic ascending arousal system of the rat. *Anesthesiology* 2006;104(1):122–33.
- [20] Zhang X, Baer AG, Price JM, Jones PC, Garcia BJ, Romero J, et al. Neurotransmitter networks in mouse prefrontal cortex are reconfigured by isoflurane anesthesia. *J Neurophysiol* 2020;123(6):2285–96.
- [21] Müller CP, Pum ME, Amato D, Schüttler J, Huston JP, Silva MA. The in vivo neurochemistry of the brain during general anesthesia. *J Neurochem* 2011;119(3):419–46.
- [22] Pfeffer CK, Xue M, He M, Huang ZJ, Scanziani M. Inhibition of inhibition in visual cortex: the logic of connections between molecularly distinct interneurons. *Nat Neurosci* 2013;16(8):1068–76.
- [23] Litwin-Kumar A, Rosenbaum R, Doiron B. Inhibitory stabilization and visual coding in cortical circuits with multiple interneuron subtypes. *J Neurophysiol* 2016;115(3):1399–409.
- [24] Hattori R, Kuchibhotla KV, Froemke RC, Komiyama T. Functions and dysfunctions of neocortical inhibitory neuron subtypes. *Nat Neurosci* 2017;20(9):1199–208.
- [25] Markram H, Toledo-Rodriguez M, Wang Y, Gupta A, Silberberg G, Wu C. Interneurons of the neocortical inhibitory system. *Nat Rev Neurosci* 2004;5(10):793–807.
- [26] Lee WC, Bonin V, Reed M, Graham BJ, Hood G, Glattfelder K, et al. Anatomy and function of an excitatory network in the visual cortex. *Nature* 2016;532(7599):370–4.
- [27] Tremblay R, Lee S, Rudy B. GABAergic interneurons in the neocortex: from cellular properties to circuits. *Neuron* 2016;91(2):260–92.
- [28] Hemmings Jr. HC, Akabas MH, Goldstein PA, Trudell JR, Orser BA, Harrison NL. Emerging molecular mechanisms of general anesthetic action. *Trends Pharmacol Sci* 2005;26(10):503–10.
- [29] Westphalen RI, Hemmings Jr. HC. Volatile anesthetic effects on glutamate versus GABA release from isolated rat cortical nerve terminals: basal release. *J Pharmacol Exp Ther* 2006;316(1):208–15.
- [30] Liu C, Zhou X, Zhu Q, Fu B, Cao S, Zhang Y, et al. Dopamine neurons in the ventral periaqueductal gray modulate isoflurane anesthesia in rats. *CNS Neurosci Ther* 2020;26(11):1121–33.
- [31] Marvin JS, Shimoda Y, Magloire V, Leite M, Kawashima T, Jensen TP, et al. A genetically encoded fluorescent sensor for in vivo imaging of GABA. *Nat Methods* 2019;16(8):763–70.
- [32] Marvin JS, Scholl B, Wilson DE, Podgorski K, Kazemipour A, Muller JA, et al. Stability, affinity, and chromatic variants of the glutamate sensor iGluSnFR. *Nat Methods* 2018;15(11):936–9.
- [33] Petersen CC, Crochet S. Synaptic computation and sensory processing in neocortical layer 2/3. *Neuron* 2013;78(1):28–48.
- [34] Morgenstern NA, Bourg J, Petreanu L. Multilaminar networks of cortical neurons integrate common inputs from sensory thalamus. *Nat Neurosci* 2016;19(8):1034–40.
- [35] Quiquempoix M, Fayad SL, Boutourlinsky K, Leresche N, Lambert RC, Bessaih T. Layer 2/3 pyramidal neurons control the gain of cortical output. *Cell Rep* 2018;24(11):2799–807 e4.
- [36] Sun W, Tan Z, Mensh BD, Ji N. Thalamus provides layer 4 of primary visual cortex with orientation- and direction-tuned inputs. *Nat Neurosci* 2016;19(2):308–15.
- [37] Yuan Y, Wu W, Chen M, Cai F, Fan C, Shen W, et al. Reward Inhibits Paraventricular CRH Neurons to Relieve Stress. *Curr Biol* 2019;29(7):1243–51 e4.
- [38] Wang F, Zhang J, Yuan Y, Chen M, Gao Z, Zhan S, et al. Salience processing by glutamatergic neurons in the ventral pallidum. *Sci Bull* 2020;65(5):389–401.
- [39] Qiu G, Wu Y, Yang Z, Li L, Zhu X, Wang Y, et al. Dexmedetomidine activation of dopamine neurons in the ventral tegmental area attenuates the depth of sedation in mice. *Anesthesiology* 2020;133(2):377–92.
- [40] Li J, Lu C, Gao Z, Feng Y, Luo H, Lu T, et al. SNRIs achieve faster antidepressant effects than SSRIs by elevating the concentrations of dopamine in the forebrain. *Neuropharmacology* 2020;177:108237.
- [41] Chemali J, Ching S, Purdon PL, Solt K, Brown EN. Burst suppression probability algorithms: state-space methods for tracking EEG burst suppression. *J Neural Eng* 2013;10(5):056017.
- [42] Li J, Li H, Wang D, Guo Y, Zhang X, Ran M, et al. Orexin activated emergence from isoflurane anaesthesia involves excitation of ventral tegmental area dopaminergic neurons in rats. *Br J Anaesth* 2019;123(4):497–505.
- [43] Yu X, Li W, Ma Y, Tossell K, Harris JJ, Harding EC, et al. GABA and glutamate neurons in the VTA regulate sleep and wakefulness. *Nat Neurosci* 2019;22(1):106–19.
- [44] Loeven AM, Receno CN, Cunningham CM, DeRuisseau LR. Arterial blood sampling in male CD-1 and C57BL/6J mice with 1% isoflurane is similar to awake mice. *J Appl Physiol* 2018;125(6):1749–59.
- [45] Janssen BJ, De Celle T, Debets JJ, Brouns AE, Callahan MF, Smith TL. Effects of anesthetics on systemic hemodynamics in mice. *Am J Physiol Heart Circulatory Physiol* 2004;287(4):H1618–24.
- [46] Kortelainen J, Jia X, Seppänen T, Thakor N. Increased electroencephalographic gamma activity reveals awakening from isoflurane anaesthesia in rats. *Br J Anaesth* 2012;109(5):782–9.
- [47] Imas OA, Ropella KM, Ward BD, Wood JD, Hudetz AG. Volatile anesthetics disrupt frontal-posterior recurrent information transfer at gamma frequencies in rat. *Neurosci Lett* 2005;387(3):145–50.
- [48] Li D, Hambrecht-Wiedbusch VS, Mashour GA. Accelerated recovery of consciousness after general anesthesia is associated with increased functional brain connectivity in the high-gamma bandwidth. *Front Syst Neurosci* 2017;11:16.
- [49] Caraiscos VB, Newell JG, You-Ten KE, Elliott EM, Rosahl TW, Wafford KA, et al. Selective enhancement of tonic GABAergic inhibition in murine hippocampal neurons by low concentrations of the volatile anesthetic isoflurane. *J Neurosci* 2004;24(39):8454–8.
- [50] de Sousa SL, Dickinson R, Lieb WR, Franks NP. Contrasting synaptic actions of the inhalational general anesthetics isoflurane and xenon. *Anesthesiology* 2000;92(4):1055–66.
- [51] Ogawa SK, Tanaka E, Shin MC, Kotani N, Akaike N. Volatile anesthetic effects on isolated GABA synapses and extrasynaptic receptors. *Neuropharmacology* 2011;60(4):701–10.
- [52] Ranft A, Kurz J, Deuringer M, Haseneder R, Dodt HU, Zieglgänsberger W, et al. Isoflurane modulates glutamatergic and GABAergic neurotransmission in the amygdala. *Eur J Neurosci* 2004;20(5):1276–80.
- [53] Petroff OA. GABA and glutamate in the human brain. *Neuroscientist* 2002;8(6):562–73.
- [54] Park J, Papoutsis A, Ash RT, Marin MA, Poirazi P, Smirnakis SM. Contribution of apical and basal dendrites to orientation encoding in mouse V1 L2/3 pyramidal neurons. *Nat Commun* 2019;10(1):5372.
- [55] Fu Y, Tucciarone JM, Espinosa JS, Sheng N, Darcy DP, Nicoll RA, et al. A cortical circuit for gain control by behavioral state. *Cell* 2014;156(6):1139–52.
- [56] Silvanto J. Is primary visual cortex necessary for visual awareness? *Trends Neurosci* 2014;37(11):618–9.
- [57] Tong F. Primary visual cortex and visual awareness. *Nat Rev Neurosci* 2003;4(3):219–29.
- [58] Pal D, Dean JG, Liu T, Li D, Watson CJ, Hudetz AG, et al. Differential Role of Prefrontal and Parietal Cortices in Controlling Level of Consciousness. *Curr Biol* 2018;28(13):2145–52 e5.
- [59] Xie Z, McMillan K, Pike CM, Cahill AL, Herring BE, Wang Q, et al. Interaction of anesthetics with neurotransmitter release machinery proteins. *J Neurophysiol* 2013;109(3):758–67.
- [60] Baumgart JP, Zhou ZY, Hara M, Cook DC, Hoppa MB, Ryan TA, et al. Isoflurane inhibits synaptic vesicle exocytosis through reduced Ca²⁺ influx, not Ca²⁺-exocytosis coupling. In: Proceedings of the national academy of sciences of the United States of America, 112; 2015. p. 11959–64.
- [61] Hemmings Jr. HC, Yan W, Westphalen RI, Ryan TA. The general anesthetic isoflurane depresses synaptic vesicle exocytosis. *Mol Pharmacol* 2005;67(5):1591–9.
- [62] Zimin PI, Woods CB, Kayser EB, Ramirez JM, Morgan PG, Sedensky MM. Isoflurane disrupts excitatory neurotransmitter dynamics via inhibition of mitochondrial complex I. *Br J Anaesth* 2018;120(5):1019–32.
- [63] Wang H, Jing M, Li Y. Lighting up the brain: genetically encoded fluorescent sensors for imaging neurotransmitters and neuromodulators. *Curr Opin Neurobiol* 2018;50:171–8.
- [64] Lee U, Ku S, Noh G, Baek S, Choi B, Mashour GA. Disruption of frontal-parietal communication by ketamine, propofol, and sevoflurane. *Anesthesiology* 2013;118(6):1264–75.
- [65] Baer AG, Bourdon AK, Price JM, Campagna SR, Jacobson DA, Baghdoyan HA, et al. Isoflurane anesthesia disrupts the cortical metabolome. *J Neurophysiol* 2020;124(6):2012–21.